buildings

MDPI

Article

Research on the Mix Proportion, Admixtures Compatibility and Sustainability of Fluidized Solidification Soil Coordinated with Multi-Source Industrial Solid Wastes

Hao Sun [1], Rong Shu [2], Jilin Liu [2], Xiaoqing Yu [3], Bolin Han [1], Xinzhuang Cui [1,*], Huaming Meng [4] and Xiaoning Zhang [4,*]

[1] School of Civil Engineering, Shandong University, Jinan 250061, China; h.sun601@foxmail.com (H.S.); hanbl96@163.com (B.H.)
[2] Gansu Academy of Building Research (Group) Co., Ltd., Lanzhou 730070, China; shurong123gsjky@163.com (R.S.); liujl123gsjky@163.com (J.L.)
[3] Jiangxi Ganyue Expressway Co., Ltd., Nanchang 330025, China; yuxiaoqing@gygs6.wecom.work
[4] School of Civil Engineering, Chongqing University, Chongqing 400045, China; mhm15957502463@163.com
* Correspondence: cuixz@sdu.edu.cn (X.C.); sdjtuzxn@163.com (X.Z.)

Abstract

To promote the resource utilization of industrial solid waste, this study developed a multi-source industrial solid waste cementitious material (MSWC) for fluidized solidified soil (FSS), which consists of steel slag (SS), granulated blast furnace slag (GBFS), circulating fluidized bed fly ash (CFBFA), desulfurization gypsum (DG) and ordinary Portland cement (OPC). Firstly, the influence of industrial solid waste contents on the unconfined compressive strength (UCS) of FSS solidified with MSWC (MSWC-FSS) was studied, and the optimal proportion for MSWC was determined as SS:GBFS:CFBFA:DG:OPC = 20:40:15:5:20. Then, the effects of water reducers (PCE and FDN) and early-strength agents (Na_2SO_4 and $CaCl_2$) on the flow expansion, setting time and UCS of MSWC-FSS were studied. With the increase of PCE and FDN, the flow expansion, setting time and UCS of MSWC-FSS increased. With the increase of Na_2SO_4 and $CaCl_2$, the flow expansion and setting time of MSWC-FSS decreased, and 3 d and 7 d UCS increased, and 28 d UCS first increased and then decreased. The best mixing scheme of water reducer and admixture is 0.5% PCE and 1% Na_2SO_4, respectively. Finally, the sustainability of MSWC-FSS was assessed. The heavy metal leaching of MSWC-FSS met the safety requirements. For FSS cementitious materials, the cost and carbon emissions of MSWC were only 43.9% and 22.4% of OPC, respectively.

Keywords: fluidized solidified soil; industrial solid waste; water reducer; early-strength agent; unconfined compressive strength; flow expansion; setting time; sustainability

check for updates

Academic Editor: Salvatore Verre

Received: 31 October 2025
Revised: 4 December 2025
Accepted: 6 December 2025
Published: 9 December 2025

Citation: Sun, H.; Shu, R.; Liu, J.; Yu, X.; Han, B.; Cui, X.; Meng, H.; Zhang, X. Research on the Mix Proportion, Admixtures Compatibility and Sustainability of Fluidized Solidification Soil Coordinated with Multi-Source Industrial Solid Wastes. *Buildings* **2025**, *15*, 4440. https://doi.org/10.3390/buildings15244440

Copyright: © 2025 by the authors. Licensee MDPI, Basel, Switzerland. This article is an open access article distributed under the terms and conditions of the Creative Commons Attribution (CC BY) license (https://creativecommons.org/licenses/by/4.0/).

1. Introduction

Soil backfilling is ubiquitous in foundation engineering—such as behind bridge abutments and retaining walls, around utility trenches, and in deep or congested excavations—where conventional layer-by-layer compaction often suffers from inadequate densification and post-construction settlement [1–4]. In contrast, fluidized solidified soil (FSS) has emerged as an effective alternative due to its self-compaction, high fluidity and ability to be pumped or chute-poured without vibration, which is particularly advantageous in confined spaces and complex geometries [5–7]. FSS is a slurry with certain fluidity prepared by adding an appropriate amount of water and cementitious materials into the engineering

residue, which is transported to the project site or directly prepared at the project site for pouring construction [8–11]. The application of FSS in China is increasing rapidly. In 2017, 100,000 m^3 FSS was used for the backfilling of the foundation trench of the comprehensive pipe gallery in Beijing Sub Center, which is the first large-scale application of FSS in China's municipal engineering. Subsequently, Chengdu, Wuhan, Shenzhen and other cities also adopted this material. From 2022 to 2023, the annual consumption of FSS in Beijing is about 1.5 million m^3. In recent years, the annual use of FSS in Chengdu has exceeded 200,000 m^3. It is estimated that the annual usage of FSS will exceed 5 million m^3 in the future in China [2,4].

Cement is the most widely used cementitious material in FSS [1]. However, the cement manufacturing industry consumes a lot of energy and non-renewable natural resources, which increases the global carbon monoxide emissions by 5~8% [12–15]. In addition, cement usually shows poor solidification effect on soil under high water content, prone to drying shrinkage cracking, affecting the long-term durability [11,16–18]. These shortcomings have prompted increasing interest in developing alternative low-carbon adhesives specifically for FSS rheological and strength requirements.

At the same time, the rapid accumulation of industrial solid waste not only occupies land, but also pollutes soil, air and groundwater, causing serious environmental problems [19,20]. Because some industrial solid wastes rich in CaO, SiO_2 and Al_2O_3 have potential pozzolanic activity, such as fly ash, coal gangue and ground granulated blast furnace slag (GBFS), or contain components in cement, such as steel slag and waste gypsum, they can be used to prepare solid waste based cementitious materials, providing a very promising way for the utilization of solid wastes [21,22].

Recently, some researches have tried to use industrial solid waste to prepare solid waste cementitious materials suitable for FSS [23]. Ma et al. used silica fume, cement and lime as raw materials to prepare FSS cementitious materials and studied the influence of silica fume replacing part of cement on the performance of FSS, and the results showed that appropriate silica fume replacement significantly alleviated the fluidity loss of FSS and improved the mechanical properties of FSS, and the optimal content of silica fume was 8%. When the water-solid ratio is 0.55, and the silica fume replacement rate is 0~12%, the 28 d unconfined compressive strength (UCS) of FSS is between 0.8~1.0 MPa [10]. Lei et al. used GBFS, fly ash, carbide slag and $Ca(OH)_2$ as raw materials to prepare composite binder suitable for loess-based FSS, and the FSS showed good application performance. When the water-solid ratio is 0.50 and the cementitious material content is 16%, the compressive strength of FSS is 1.5 MPa [2]. Zhang et al. studied the effects of municipal solid waste incineration bottom residue (MSWI-BA) and MSWI-BA powder (MSWI-BAP) as fine aggregate and cementitious material components on FSS, and the results showed that the volume deformation of FSS with MSWI-BA and MSWI-BAP increased, but the development of mechanical strength was not affected. When the water-solid ratio is about 0.6 and the cementitious material content is 30%, the 28 d UCS of FSS is between 3~7 MPa [3,7]. Sun et al. used alkali-activated GBFS and cement as cementitious material, shield tunnel spoil as matrix, and added anti-washout admixtures to prepare FSS suitable for underwater filling, which showed good underwater performance. After adding anti-dispersant, the 28 d UCS of FSS formed in air is about 1.5~1.6 MPa, and the 28 d UCS of FSS formed in water is 1.35 MPa [6]. Liu et al. prepared cementitious material with composite alkali activator (CaO and Na_2CO_3) and GBFS as raw materials, and studied the influence of cementitious material content on the performance of FSS, and the results showed that with the increase of cementitious material content, the fluidity of FSS first increased and then decreased, and the UCS of FSS increased. When cementitious material content increased from 30% to 50%, the 28 d UCS of FSS increased from 4.4 MPa to 7.3 MPa [9]. Liu et al. used CaO, cement and fly ash as raw materials

to prepare the cementitious material suitable for FSS, and the results showed that when the ratio of fly ash and CaO was 1:1, the 28 d UCS of FSS with a sand ratio of 2% was the highest, reaching 0.9 MPa. With the increase of sand ratio from 2% to 65%, the 28 d UCS of FSS gradually increases to about 3.3 MPa [5]. The multi-source solid waste cementitious materials (MSWC) prepared with 3–4 kinds of industrial solid wastes tend to have better curing effect on FSS, because this method plays a coordinating role among various industrial solid wastes. Feng et al. prepared FSS with cement, fly ash, GBFS, desulfurization gypsum (DG) and high moisture content slurry from the construction site, and found that the mechanical properties of FSS were the best under the mix proportion of 30% cement, 10% fly ash, 40% GBFS and 20% DG, and the 28 d UCS could reach 0.67 MPa [8]. Xiao et al. used GBFS, circulating fluidized bed fly ash (CFBFA), DG and cement as raw materials to prepare MSWC suitable for loess-based FSS, and recommended the mix proportion of composite cementitious materials as follows: at 10% cement, the proportional range of GBFS, CFBFA and DG were 43–50%, 25–32% and 8–15%, respectively. Within this ratio range, the 28 d UCS of FSS was greater than 1.2 MPa [23]. Gu et al. prepared MSWC for FSS with GBFS, fly ash, carbide slag, cement and DG. The fluidity of FSS was more than 350 mm, and the 28 d UCS was more than 3 MPa [24]. A summary of the research on FSS using solid waste cementitious materials is shown in Table 1.

Table 1. Mix proportion and strength of FSS using solid waste cementitious materials.

References	Raw Materials of Cementitious Material	Soil	Admixtures	Mass Ratio of Cementitious Material to Dry Soil (%)	Water-Solid Ratio	28 d UCS of FSS (MPa)	Size of UCS Specimen (mm)
[10]	Cement, silica fume and CaO	Dredged sediment	/	20	0.55	0.8~1.0	70.7 × 70.7 × 70.7
[2]	GBFS, fly ash, carbide slag and $Ca(OH)_2$	Low-plasticity clay	/	8, 12, 16, 20	0.50, 0.52, 0.54, 0.56, 0.58	0.3~2.4	φ39.1 × 80
[3,7]	GBFS, MSWI-BAP, cement, gypsum and sodium silicate	Clay mixed with MSWI-BA aggregate	1.5% water reducer	30	About 0.6	3~7	φ40 × 80
[6]	Sodium silicate, GBFS and cement	Waste shield tunnelling soil	Anti-washout admixtures (polyacrylamide, hydroxyethyl cellulose), 0.075% PCE	23	0.967	1.5~1.6 (formed in air), 1.35 (formed in water)	φ39.1 × 80
[9]	alkaline-activator (CaO and Na_2CO_3), GBFS	The soil from the foundation trench	/	30, 35, 40, 45, 50	0.67	4.4~7.3	70.7 × 70.7 × 70.7
[5]	CaO, cement and fly ash	Engineering excavated soil mixed with 2%, 15% and 65% sand	/	15	0.8	0.4~3.3	100 × 100 × 100
[8]	Cement, fly ash, GBFS and DG	High moisture content slurry from the construction site	2% water reducer	16.3	0.542	0.67	70.7 × 70.7 × 70.7
[23]	Cement, GBFS, CFBFA and DG	Loess	/	15	0.51	0.39~2.14	70.7 × 70.7 × 70.7
[24]	GBFS, fly ash, carbide slag, cement and DG	The soil from a construction site	0.5% water reducers (FDN and PCE), 1.5% early-strength agents (NaCl, $CaCl_2$ and Na_2SO_4)	25	0.32	3~6	40 × 40 × 160

Admixtures are widely used in concrete and mortar, and the performance of concrete and mortar can be effectively adjusted by using a small amount of admixtures [25–27]. A few studies reported the attempt to apply admixtures to FSS. Sun et al. studied the influence of two anti-washout admixtures, polyacrylamide and hydroxyethyl cellulose, on the performance of geopolymer based FSS. The study found that with the increase of anti-washout admixture content, the flow value of FSS decreased significantly, UCS of FSS formed in air improved slightly, the resistance to water erosion improved significantly, and the composite effect of the two anti-washout admixtures was better [6]. Gu studied the influence of different types of water reducer (naphthalene superplasticizer and polycarboxylate superplasticizer) and early-strength agent (NaCl, $CaCl_2$ and Na_2SO_4) on the performance of FSS. The content of water reducer and early-strength agent were 0.5% and 1.5% of the cementitious material of FSS, respectively. The results show that both naphthalene superplasticizer (FDN) and polycarboxylate superplasticizer (PCE) can improve the compressive strength and fluidity of FSS, and PCE has better effect on improving the fluidity of FSS; Three kinds of early-strength agents can significantly improve the early strength of FSS, and Na_2SO_4 has the best effect, followed by $CaCl_2$, and finally NaCl [24]. Zhang [3,7] and Feng [8] added a small amount of water reducing agent to the material composition of FSS, but did not further analyze the impact of these water reducing agents on FSS.

Although the current research has made some achievements, there are still some problems. (1) There are few kinds of industrial solid wastes in the study of FSS, and whether other kinds of industrial solid wastes can be applied in FSS needs further study, such as steel slag (SS). SS is a kind of solid waste produced in the process of steelmaking. China's annual output of crude steel accounts for about half of the world's annual output of crude steel, so China's annual output of SS has reached an astonishing 120 million tons, but the comprehensive utilization rate is about 20~30% [22,28]. The main chemical composition and mineral phase of SS are similar to that of Portland cement clinker, so SS has potential cementitious properties and is called poor cement clinker [22,28–34]. If SS can be used as a component of FSS cementitious material, the comprehensive utilization rate of SS can be effectively improved. (2) There are few studies on the influence of admixtures on FSS, and the research is not comprehensive. For example, it is not clear how the amount of admixtures affects the performance of FSS, how the admixtures affect the setting time and durability of FSS, and whether the admixtures are applicable to FSS using other types of solid waste cementitious materials. (3) There are many studies on the performance of FSS using solid waste cementitious materials, but less analysis on sustainability and safety of FSS using solid waste cementitious materials.

Considering the aforementioned factors, this study developed a MSWC for FSS, which mainly consists of SS, GBFS, CFBFA, DG and ordinary Portland cement (OPC). Firstly, the influence of industrial solid waste contents on the UCS of FSS solidified with MSWC (MSWC-FSS) was studied to determine the optimal mix proportion of MSWC. Then, the effects of two water reducers (FDN and PCE) and two early-strength agents (Na_2SO_4 and $CaCl_2$) on the flow expansion, setting time, and UCS of MSWC-FSS in the optimal MSWC mix proportion were studied. Finally, the sustainability of MSWC-FSS was evaluated through heavy metal leaching test, cost analysis and carbon emissions analysis.

2. Materials and Methods

2.1. Experimental Materials

2.1.1. Soil

The soil used in this study was obtained from a construction site in Jinan City, China. The soil is widely distributed across the Yellow River alluvial plain (Figure 1), which is

light yellow, fine particle size, loose structure, difficult to be compacted in the project, and has poor water stability [35–37]. The particle size distribution curve and the basic physical properties of the soil are shown in Figure 2. The test results indicate that the soil belongs to low liquid limit silt. The soil exhibits a relatively high coefficient of uniformity (C_u = 11.5) and a coefficient of curvature (C_c = 2.1), suggesting favorable gradation and suitable engineering properties. The particle size distribution shows a steep curve, with most particles concentrated in the 20–100 μm range, and the clay fraction (particles smaller than 5 μm) accounts for less than 10%.

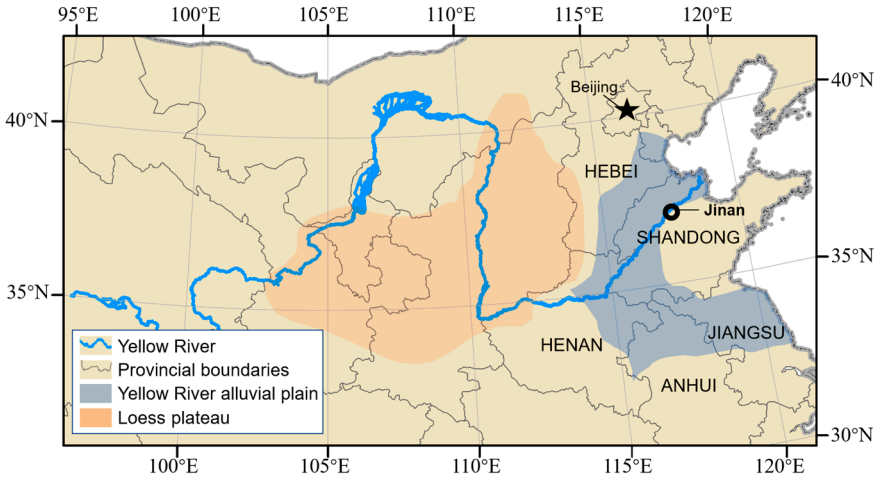


Figure 1. Location of soil sample.

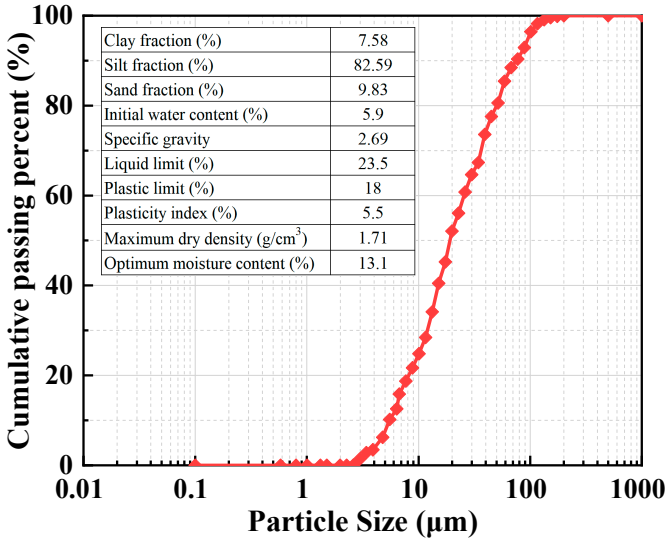


Figure 2. Gradation curve of the soil.

2.1.2. Raw Materials of MSWC

The MSWC were prepared from five raw materials: SS, GBFS, CFBFA, DG, and OPC. The SS was collected from Laiwu Iron and Steel Group Co., Ltd. (Jinan City, China). The GBFS (Grade S95) was obtained from a local ironmaking plant (Jinan City, China). The CFBFA and DG were collected from a thermal power plant (Ningbo City, China). The OPC (P.O 42.5) was provided by Shanshui Cement Co., Ltd. (Jinan City, China), and its basic parameters are shown in Table 2. The appearance of various raw materials is shown in Figure 3. MSWC was prepared by mixing the five raw materials evenly in the mixer.

Table 2. Basic parameters of OPC.

Setting Time (min)		Compressive Strength (MPa)			Specific Surface Area (m^2/kg)
Initial	Final	3 d	7 d	28 d	
115	184	33.8	43.5	51.6	381



Figure 3. Appearance of various raw materials.

The particle size distribution curves of the raw materials measured by laser particle size analyzer are shown in Figure 4. The median particle diameters (d_{50}) of SS, GBFS, CFBFA, DG, and OPC were 9.71 μm, 6.68 μm, 4.26 μm, 11.28 μm, and 8.44 μm, respectively. The effective particle diameters (d_{10}) were 2.11 μm, 1.13 μm, 0.68 μm, 2.79 μm, and 1.86 μm, respectively, indicating that CFBFA had the finest particles, while DG had the coarsest.

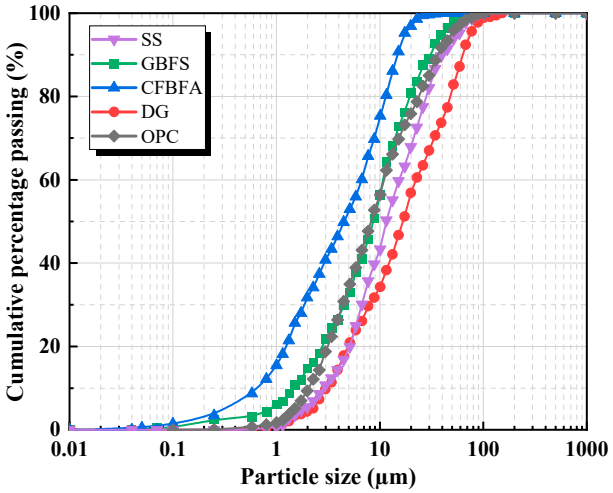


Figure 4. Particle size characteristic curve of raw materials.

The chemical and mineral compositions of all raw materials were analyzed using X-ray fluorescence and X-ray diffraction analysis, as presented in Table 3 and Figure 5. The main chemical compositions of SS are CaO, SiO_2, Al_2O_3 and Fe_2O_3. The main chemical compositions of GBFS and OPC are CaO, SiO_2, and Al_2O_3. The main chemical compositions

of CFBFA are SiO_2, and Al_2O_3. The main chemical compositions of DG are CaO and SO_3. The chemical composition of SS includes the composition of cement clinker such as tricalcium silicate (C_3S) and dicalcium silicate (C_2S) and a small amount of RO phase (oxide solid solution of Mg^{2+}, Fe^{2+}, Mn^{2+}) and f-CaO, indicating high pozzolanic activity [22,38]. GBFS has no obvious diffraction peaks, characteristic of an amorphous glassy phase, with a small number of crystalline calcium–aluminosilicate phases superimposed. CFBFA mainly contains quartz (SiO_2), hematite (Fe_2O_3), and albite ($NaAlSi_3O_8$). DG consists primarily of calcium sulfate ($CaSO_4$) and gypsum ($CaSO_4 \cdot 2H_2O$). The mineral phases of OPC are dominated by C_3S and C_2S.

Table 3. Chemical composition of raw materials.

Materials	Chemical Composition (wt.%)							
	CaO	**SiO_2**	**Al_2O_3**	**MgO**	**Fe_2O_3**	**SO_3**	**TiO_2**	**K_2O**
SS	30.62	16.28	8.72	6.29	28.57	—	—	—
GBFS	44.71	29.29	14.85	7.33	0.39	1.28	0.68	0.41
CFBFA	3.44	49.93	36.17	0.79	5.8	1.12	1.01	1.17
DG	45.35	1.56	0.8	0.35	0.12	50.63	0.02	0.41
OPC	51.42	24.99	8.26	3.71	4.03	2.51	—	—

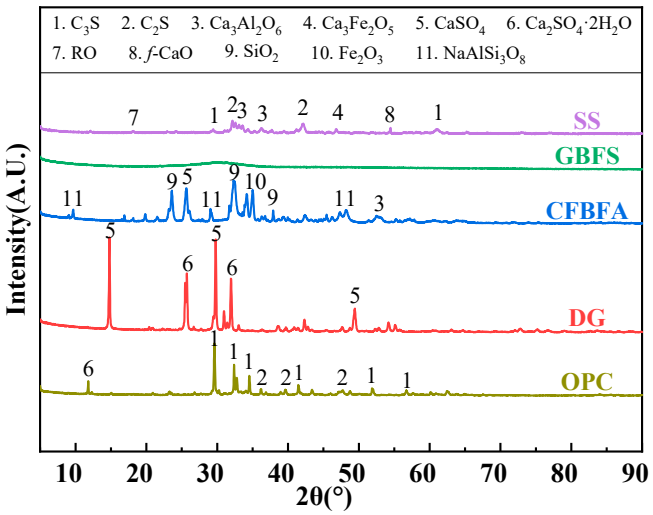


Figure 5. Mineral compositions of raw materials.

2.1.3. Admixtures

The two water reducers used in this study are FDN and PCE, which were purchased from Shandong Yousuo Chemical Technology Co., Ltd. (Linyi City, China). The two early-strength agents used in this study are sodium sulfate (Na_2SO_4) and calcium chloride ($CaCl_2$), both of which are purchased from China National Pharmaceutical Group Co., Ltd. (Shanghai City, China), with a purity of analytical reagent grade.

2.2. Experimental Methods

2.2.1. MSWC-FSS Preparation

SS, GBFS, CFBFA, DG and OPC are uniformly mixed into MSWC according to different mix proportions. MSWC-FSS is prepared by mixing MSWC, dried soil and admixture together and mixing them evenly in a slurry mixer. Based on preliminary experiments and engineering experience, the MSWC content of all FSS in this study is 15 wt.% and the water-solid ratio is 0.45. In the development of MSWC for FSS, the mix proportion scheme of MSWC is shown in Table 4, and no admixture is added. In the study of compatibility of

admixtures with MSWC-FSS, the content scheme of admixtures is shown in Table 5, and the optimal mix proportion of MSWC is adopted. The content of MSWC and admixture is the mass ratio of MSWC or admixture to dry soil. The preparation process MSWC-FSS is shown in Figure 6.

Table 4. Mix proportion scheme of MSWC.

Number	Raw Materials Content in MSWC (wt.%)					MSWC Content (wt.%)	Water-Solid Ratio
	SS	GBFS	CFBFA	DG	OPC		
1	10	35	10	5	40	15	0.45
2	15	35	10	5	35		
3	20	35	10	5	30		
4	25	35	10	5	25		
5	30	35	10	5	20		
6	15	20	10	5	50		
7	15	30	10	5	40		
8	15	40	10	5	30		
9	15	50	10	5	20		
10	15	60	10	5	10		
11	15	35	5	5	40		
12	15	35	10	5	35		
13	15	35	15	5	30		
14	15	35	20	5	25		
15	15	35	25	5	20		
16	15	35	10	2	38		
17	15	35	10	4	36		
18	15	35	10	6	34		
19	15	35	10	8	32		
20	15	35	10	10	30		

Table 5. Content scheme of admixtures.

Admixture Content (%)		MSWC Content (wt.%)	Water-Solid Ratio
Water Reducers (FDN and PCE)	Early-Strength Agents (Na_2SO_4 and $CaCl_2$)		
0.5, 1, 1.5	0	15	0.45
0	0.5, 1, 1.5		

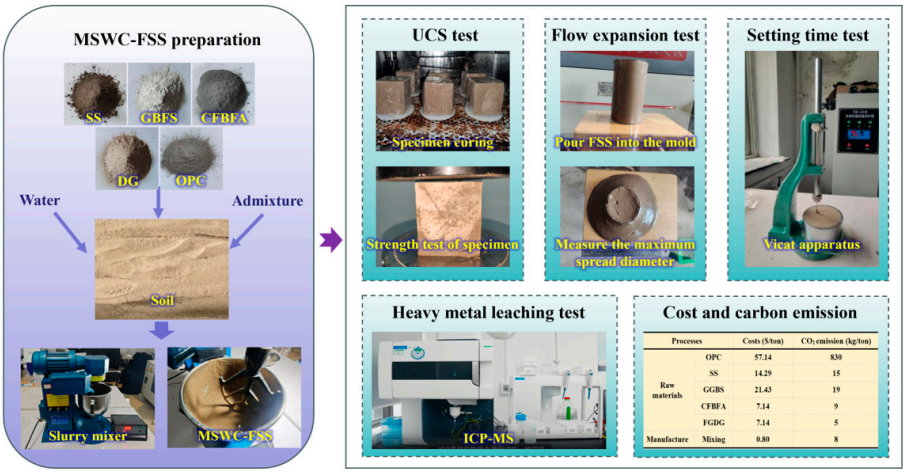


Figure 6. FSS specimen preparation and test process.

2.2.2. UCS Test

The UCS test of MSWC-FSS was conducted in accordance with the Chinese standard JTG 3430-2020 [39], and the steps are as follows. First, the freshly mixed MSWC-FSS was poured into a cubic mold with the size of 70.7 mm × 70.7 mm × 70.7 mm. The surface was leveled, the mold was wrapped with plastic film, and the sample was placed in a curing box. Secondly, after 2 days of curing, the specimen was demolded, wrapped again with plastic film, and returned to the curing box until the specified curing ages of 3, 7 and 28 days were reached. The curing conditions in curing box were maintained at 20 °C and 96% humidity. Finally, the specimens of MSWC-FSS that had reached the curing time were taken out of the curing box and tested. The tests were carried out using a WDW-100 universal testing machine (produced by Jinan Dongce Testing Equipment Co., Ltd., Jinan, China) under a constant loading rate of 1 mm/min. Each test group consisted of three parallel specimens, and the arithmetic mean value of the results was taken as the final UCS. The UCS test process is shown in Figure 6.

2.2.3. Flow Expansion Test

The flow expansion test of MSWC-FSS was conducted according to ASTM D6103-2017 [40] and Chinese standard DBJ51/T 188-2022 [41]. A cylindrical mold with an inner diameter of 75 mm, an outer diameter of 85 mm, and a height of 150 mm was placed on a smooth glass plate placed horizontally, and the freshly mixed MSWC-FSS was filled into the mold until full. The surface was leveled, and the mold was then lifted vertically at a uniform rate, allowing the mixture to collapse freely under gravity and spread into a circular shape. The maximum spread diameters along two perpendicular directions were measured, and their arithmetic mean was recorded as the flow expansion value of the material. The testing process is shown in Figure 6.

2.2.4. Setting Time Test

The setting time test of of MSWC-FSS was conducted according to Chinese standard GB/T 1346-2024 [42]. The same procedure used for cement paste testing was applied to determine the initial and final setting times of MSWC-FSS by Vicat apparatus. The testing process is shown in Figure 6.

2.2.5. Heavy Metal Leaching Test

According to Chinese specification GB 5085.3-2007 and HJ/T 299-2007 [43,44], heavy metal leaching test was conducted to study the leaching of heavy metal ions from the solidified waste in the MSWC-FSS. The experimental equipment included an Inductively Coupled Plasma Mass Spectrometer (ICP-MS NexION 1000G, PerkinElmer, Shanghai, China) and an Atomic Fluorescence Spectrometer (AFS-933, Beijing Titan Instrument Co., Ltd., Beijing, China). The experimental equipment is shown in Figure 6.

3. Development of MSWC for FSS

When various types of industrial solid wastes are combined, their chemical composition and mineral phase can produce synergistic and complementary effects [1,2,23]. This part studies the influence of different industrial solid waste mixing ratio on the UCS of MSWC-FSS, in order to determine the optimal mix proportion of each component in MSWC.

3.1. Effect of SS Content on UCS of MSWC-FSS

Figure 7 shows the effect of different SS content on 7-day and 28 day UCS of MSWC-FSS. The 7-day and 28 day UCS of MSWC-FSS increased first and then decreased with

the increase in SS content. When the SS content was about 20%, the UCS reached the maximum value, and the strength was 0.60 MPa at 7 d and 0.96 MPa at 28 d. The strength enhancement of MSWC-FSS with appropriate SS content is mainly attributed to the presence of active minerals in SS, such as C_3S and C_2S [22,28,29,34]. The hydration of OPC in MSWC produces OH^-, which promotes the dissolution and reaction of active minerals in SS, and generates more hydration products, such as calcium silicate hydrate (C-S-H) and ettringite (AFt) [1,22,45]. These hydration products fill pores and bond soil particles together to form a denser microstructure and improve strength. When SS content exceeded 20%, UCS began to decline. This is because the OH^- generated by cement hydration is not enough to stimulate the dissolution of all active minerals in SS at a higher SS content, and too many SS particles do not react, which reduces the compactness and integrity of the MSWC-FSS [46].

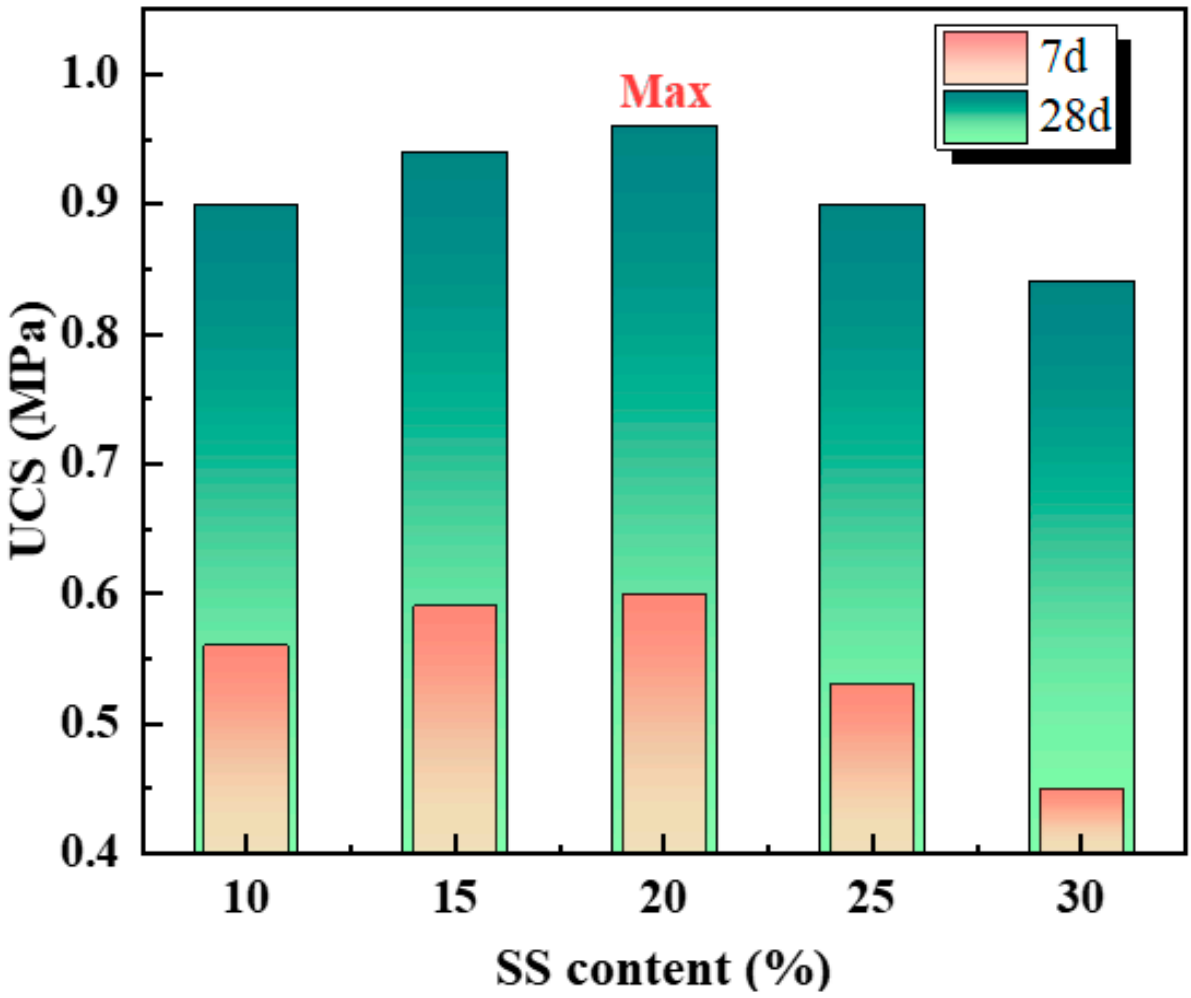


Figure 7. UCS of MSWC-FSS with different SS content.

3.2. Effect of GBFS Content on UCS of MSWC-FSS

Figure 8 shows the effect of different GBFS content on 7-day and 28 day UCS of MSWC-FSS. With the increase of GBFS content, the UCS of MSWC-FSS at 7 days and 28 days first increased and then decreased. When the GBFS content was about 40%, the UCS reached the maximum value, and the strength was 0.62 MPa at 7 d and 0.95 MPa at 28 d. Rich in amorphous aluminosilicate glassy phases, GBFS possesses strong latent hydraulic activity once sufficient alkalinity is provided [18,19]. At moderate contents (<40%), the alkaline environment generated by the hydration of calcium-bearing minerals—particularly from OPC and SS—was capable of activating the depolymerization of the

glassy network in GBFS. The released Si^{4+} and Al^{3+} species combined with Ca^{2+} to form C-S-H and calcium aluminate hydrate (C-A-H) gels, which progressively filled pores and strengthened interparticle bonding, thus improving the integrity of the soil matrix [18,19,47]. In contrast, further increasing the GBFS content beyond 40% led to a gradual decline in UCS. The excessive incorporation of slag consumed available alkaline activators, reducing the system's pH and hindering continued dissolution of the amorphous phase. Consequently, part of the GBFS remained unreacted, resulting in a less compact microstructure and incomplete hydration.

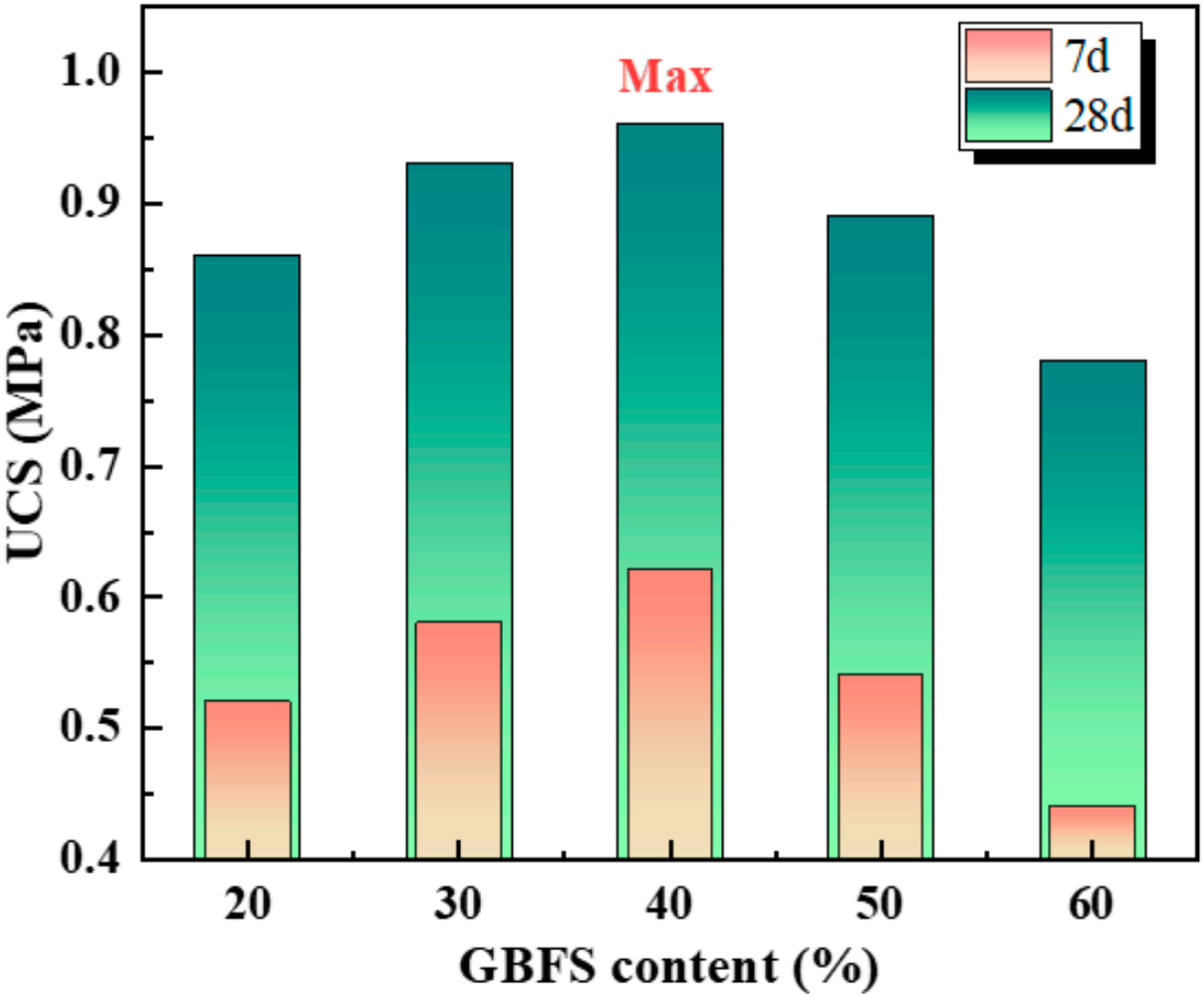


Figure 8. UCS of MSWC-FSS with different GBFS content.

3.3. Effect of CFBFA Content on UCS of MSWC-FSS

Figure 9 shows the effect of different CFBFA content on 7-day and 28 day UCS of MSWC-FSS. With the increase of CFBFA content, the UCS of MSWC-FSS at 7 days and 28 days first increased and then decreased. When the CFBFA content was about 15%, the UCS reached the maximum value, and the strength was 0.61 MPa at 7 d and 0.94 MPa at 28 d. CFBFA is rich in active SiO_2 and active Al_2O_3, especially the high content of active Al_2O_3, which reacts with OH^- produced by cement hydration to form C-S-H and C-A-H gels [19,21,48–50]. These products densify the soil matrix and improve the mechanical strength. However, excessive addition of CFBFA will consume available alkaline activators and introduce unreacted particles, reducing the overall compactness, thus slightly weakening the UCS at higher contents.

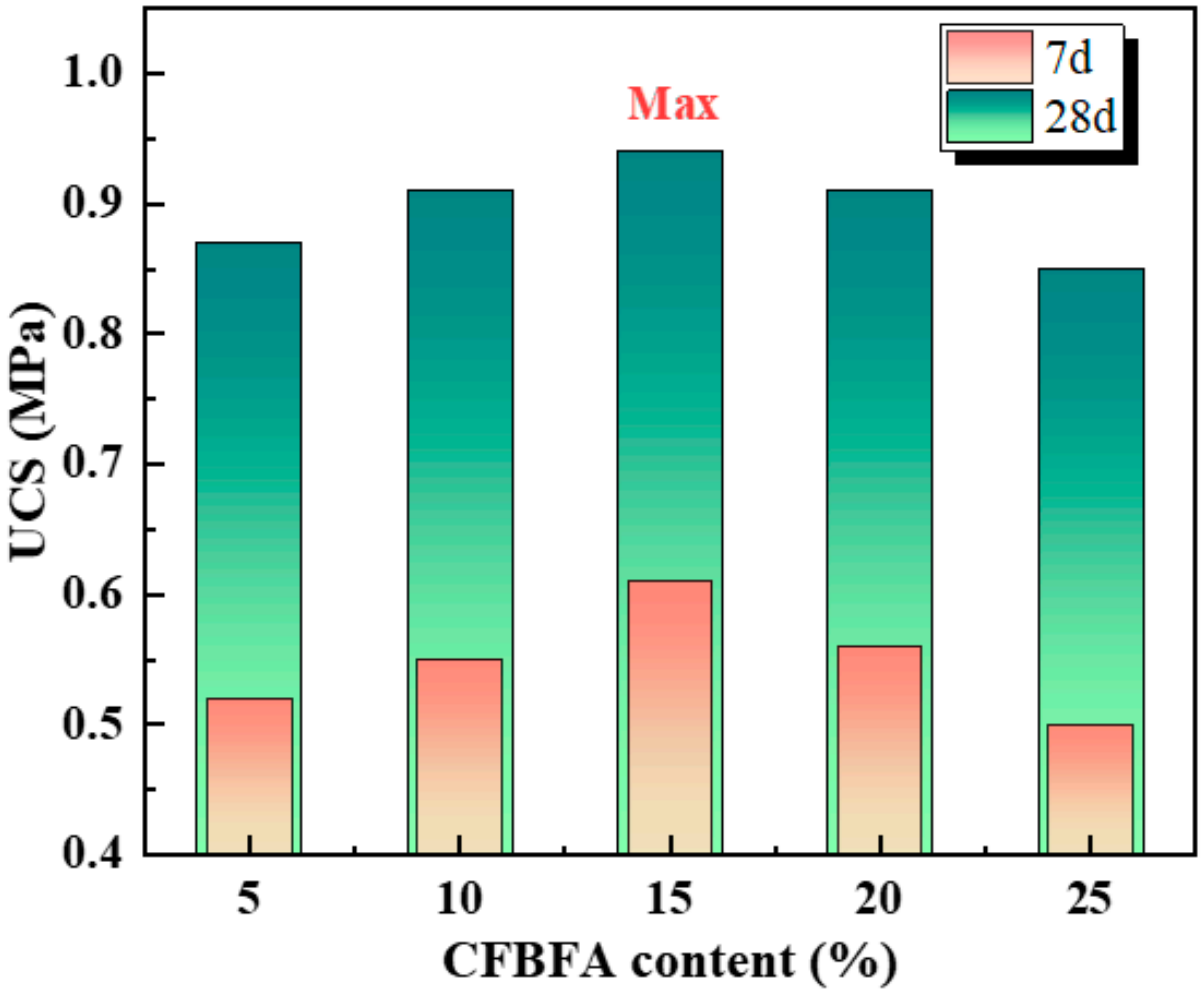


Figure 9. UCS of MSWC-FSS with different CFBFA content.

3.4. Effect of DG Content on UCS of MSWC-FSS

Figure 10 shows the effect of different DG content on 7-day and 28 day UCS of MSWC-FSS. With the increase of DG content, the UCS of MSWC-FSS at 7 days and 28 days first increased and then decreased. When the DG content was about 6%, the UCS reached the maximum value, and the strength was 0.59 MPa at 7 d and 0.90 MPa at 28 d. In the alkaline environment formed by the hydration of MSWC, SO_4^{2-} released from DG reacts with C-A-H produced by the hydration of MSWC to form AFt, which is an expanded hydration product to fill the voids and improve particle binding [18,51,52]. When the DG content exceeds the optimal value, excessive SO_4^{2-} depletes the C-A-H produced by the hydration of MSWC, and the excess SO_4^{2-} cannot further participate in the reaction to form AFt. Therefore, the intensity development rate remains almost unchanged, and the return provided by excessive DG decreases.

According to the above single factor test results, considering the strength and the convenience of MSWC preparation, the optimal mix proportion of the MSWC was determined as 20 wt.% SS, 40 wt.% GBFS, 15 wt.% CFBFA, 5 wt.% DG and 20 wt.% OPC. This composition ensures a balanced hydration reaction environment, achieving high mechanical strength while maintaining good fluidity for practical field applications. The optimal mix proportion of MSWC is adopted in the following studies.

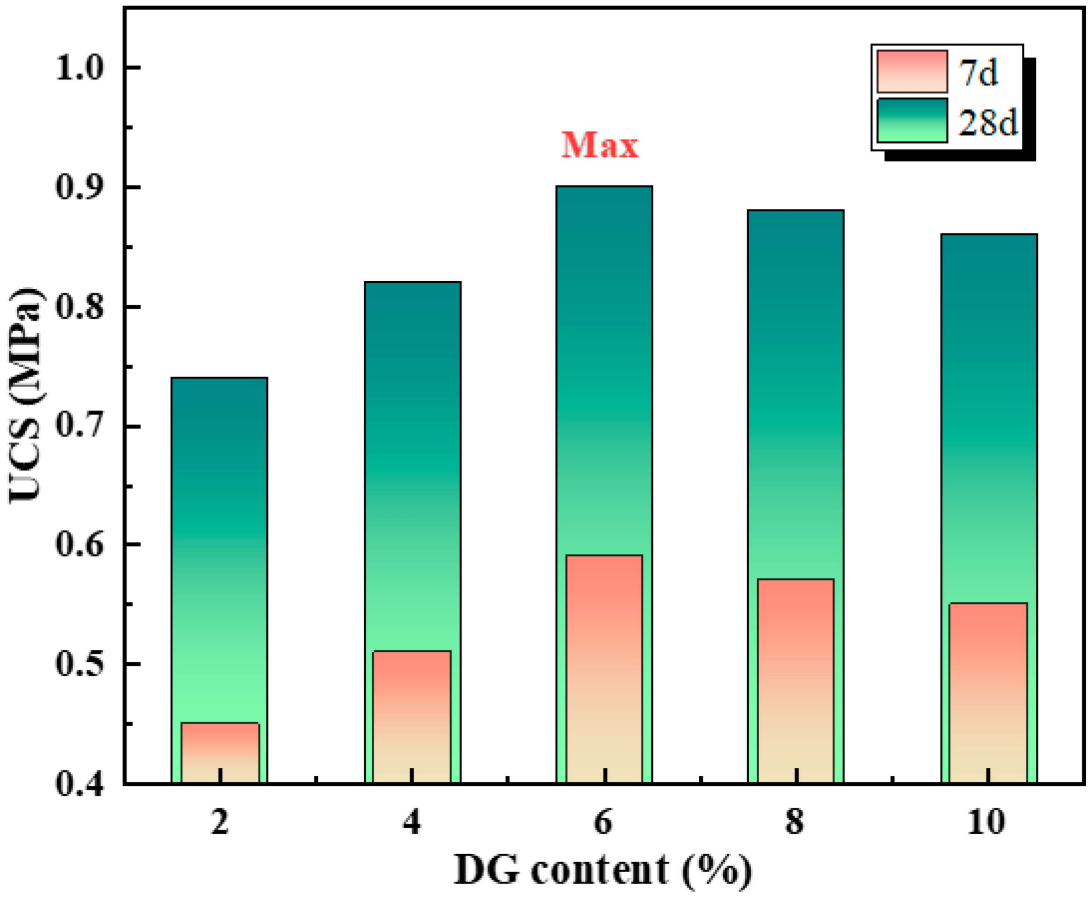


Figure 10. UCS of MSWC-FSS with different DG content.

4. Study of Compatibility of Admixtures with MSWC-FSS

4.1. Water Reducers

FSS needs greater fluidity to ensure convenient construction and transportation. Increasing the water-solid ratio is the easiest way to improve the fluidity of FSS, but it will cause significant adverse effects on its mechanical and durability properties. Water reducers can effectively reduce the mixing water volume, and at a reasonable content, it has little or even positive effect on the properties of FSS. Therefore, the following part studies the influence of water reducer on several important properties of MSWC-FSS.

4.1.1. Effect of Water Reducers on the Flow Expansion of MSWC-FSS

Figure 11 shows the influence of different content of water reducers (FDN and PCE) on the flow expansion of MSWC-FSS. With the increase of the content of the two kinds of water reducers, the flow expansion of the MSWC-FSS increases, but the growth rate gradually slows down. The influence of two water reducers on the flow expansion is extremely significant. When the contents of water reducers are 1.5%, FDN and PCE can increase the flow expansion of MSWC-FSS by 28.14% and 36.18% respectively. According to the Chinese standard DBJ51/T 188-2022, the flow expansion of FSS used for backfilling abutment, culvert and foundation trench should generally be between 160 and 220 mm, and the flow expansion of FSS requiring large fluidity should be ≥220 mm [41]. MSWC-FSS without water reducer meets the construction requirements of general fluidity (160~220 mm), and the MSWC-FSS with water reducers content ≥ 0.5% meet the construction requirements of large fluidity (≥220 mm). The mechanism of water reducers to increase the fluidity is to increase the spacing of soil particles, hinder the aggregation of particles, and release the wrapped free water [25]. Compared with FDN, the electrostatic repulsion force of PCE with

high charge density is greater, which destroys the "card house" structure formed in the static state of MSWC-FSS, with significant spatial resistance effect, thus releasing a large amount of free water and greatly improving the rheological properties of MSWC-FSS [26,53,54].

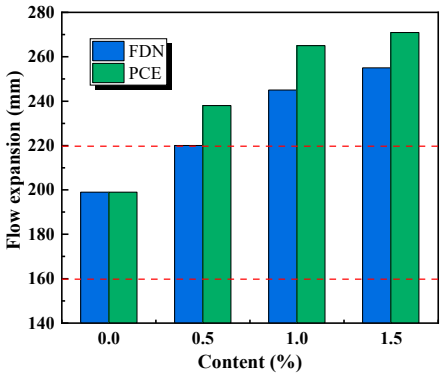


Figure 11. Flow expansion of MSWC-FSS with different water reducer content.

4.1.2. Effect of Water Reducers on the Setting Time of MSWC-FSS

Figure 12 shows the influence of different content of water reducers (FDN and PCE) on the setting time of MSWC-FSS. With the increase of the content of the two kinds of water reducers, the initial setting and final setting time of MSWC-FSS increased significantly. The retarding effect of PCE is obviously better than that of FDN, especially when the content of PCE reaches 1.5%, the initial setting time is more than doubled, which has a great impact on the construction efficiency of the project. According to the Chinese standard DBJ51/T 188-2022, the initial setting time of FSS should be greater than 45 min, and the final setting time should be less than 720 min [41]. In the actual engineering process, in order to shorten the construction period and speed up the construction, the initial setting time is usually expected to be less than 300 min. All MSWC-FSS meet the requirement that the initial setting time is greater than 45 min, and the initial setting time of MSWC-FSS mixed with water reducer cannot meet the requirement of rapid construction (<300 min). Only MSWC-FSS without water reducer and with 5% FDN meet the requirements of final setting time (<720 min). The reason for the longer setting time is that the water reducer molecules adsorb on the surface of MSWC particles to form a protective film, which limits the direct contact between MSWC particles and water and delays the occurrence and development of hydration reaction [25,26,53,54].

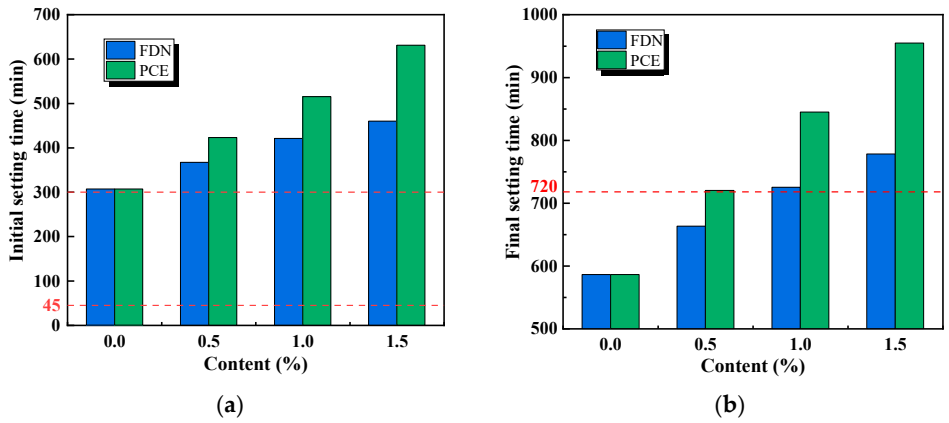


Figure 12. Setting time of MSWC-FSS with different water reducer content: (**a**) Initial setting time; (**b**) Final setting time.

4.1.3. Effect of Water Reducers on the UCS of MSWC-FSS

Figure 13 shows the influence of different content of water reducers (FDN and PCE) on the UCS of MSWC-FSS. With the increase of the content of the two kinds of water reducers, the UCS of MSWC-FSS cured for 3 d, 7 d and 28 d increased significantly. The enhancement effect of FDN on the UCS of MSWC-FSS is better than that of PCE on the whole, and this advantage is most obvious at 3 d of curing. The reason for UCS enhancement is that the water reducer increases the fluidity of MSWC-FSS, promotes the more uniform dispersion of MSWC particles in water, accelerates the hydration reaction of MSWC, makes the hydration products more evenly distributed in the soil, and produces a more continuous and stable cementitious network [26,53–55]. In addition, the improved fluidity enables the hydration products of MSWC to more effectively fill the interspace between particles in the soil, thus reducing the total porosity and average pore size, thus forming a denser MSWC-FSS [25,26,55]. According to the Chinese standard DBJ51/T 188-2022, the 28 day UCS of the FSS used for backfilling the back of abutment, retaining wall and culvert should not be less than 0.8 MPa, and the 28 day UCS of the FSS used for filling subgrade should not be less than 1.0 MPa [41]. In this study, the 28 day UCS of MSWC-FSS with all water reducer contents met the requirements.

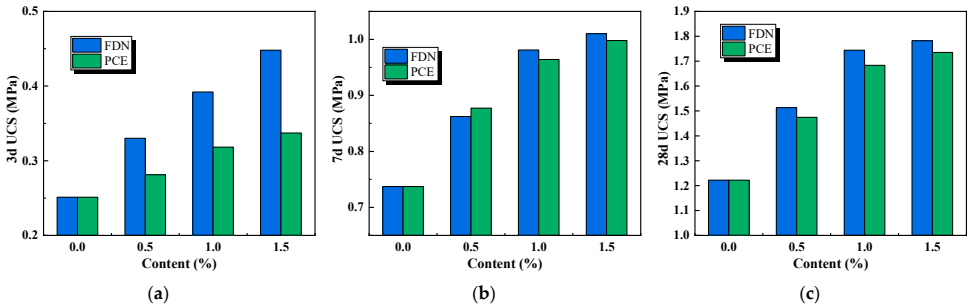


Figure 13. UCS of MSWC-FSS with different water reducer content: (**a**) Curing for 3 days; (**b**) Curing for 7 days; (**c**) Curing for 28 days.

In conclusion, both water reducers can effectively improve the flow expansion and UCS of MSWC-FSS, and significantly extend the setting time. PCE has a better enhancement effect on the fluidity of FSS, but PCE significantly increases the setting time of MSWC-FSS, especially the final setting time, which is not conducive to rapid construction; Compared to PCE, FDN has a slightly poorer effect on MSWC-FSS flow rate, but FDN does not significantly increase the setting time and has a better effect on improving UCS of MSWC-FSS, especially the 3 d UCS. Considering the requirements of engineering performance, construction capacity and cost-effectiveness, 0.5% FDN is determined as the best choice, which meets the requirements of fluidity, setting time (initial setting time > 45 min, final setting time < 720 min) and UCS.

4.2. Early-Strength Agents

Current technical specifications generally stipulate that 28 day UCS is the strength control index of FSS. However, in practical engineering applications, especially when the construction schedule is very tight, the early-strength of FSS is equally important to ensure structural stability and meet the schedule requirements. Therefore, the influence of early-strength agent on the basic properties of MSWC-FSS is studied in the following part.

4.2.1. Effect of Early-Strength Agents on the Flow Expansion of MSWC-FSS

Figure 14 shows the influence of different content of early-strength agents (Na_2SO_4 and $CaCl_2$) on the flow expansion of MSWC-FSS. With the increase of the content of the

two kinds of early-strength agents, the flow expansions of MSWC-FSS decrease. The flow expansion of all MSWC-FSS mixed with early-strength agent is more than 160 mm, which still meets the general fluidity requirements of Chinese standard DBJ51/T 188-2022 [41]. The decrease of fluidity is attributed to the promoting effect of early-strength agent on the hydration and pozzolanic reaction of MSWC, which makes MSWC form more early cementitious substances and consume some free water, thus reducing the fluidity of MSWC-FSS [27,56–59].

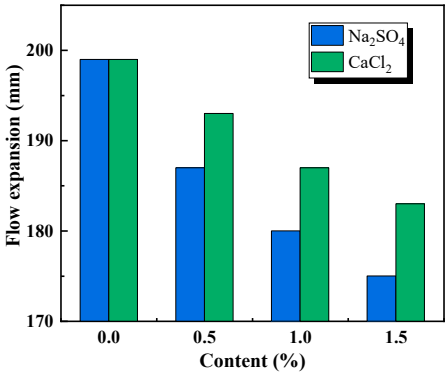


Figure 14. Flow expansion of MSWC-FSS with different early-strength agent content.

4.2.2. Effect of Early-Strength Agents on the Setting Time of MSWC-FSS

Figure 15 shows the influence of different content of early-strength agents (Na_2SO_4 and $CaCl_2$) on the setting time of MSWC-FSS. When the content is not less than 1.0%, both of the two early-strength agents meet the requirements (45 min < initial setting time < 300 min, final setting time < 720 min) of FSS rapid construction in Chinese standard DBJ51/T 188-2022 [41]. With the increase of Na_2SO_4 content, the initial setting time and final setting time of FSS gradually decreased. With the increase of $CaCl_2$ content, the initial setting time of FSS first increased and then decreased, and the final setting time gradually decreased. The essence of early-strength agent is to promote the hydration reaction, and the mechanism of action of the two early-strength agents is slightly different. Na_2SO_4 mainly reacts with C-A-H to form AFt, thus promoting the formation of early gel. It also increases the concentration of calcium ion (Ca^{2+}), promotes the rapid development of early hydration products, and makes MSWC-FSS set and harden faster [27,56,57]. $CaCl_2$ shortens the setting time by accelerating the hydration reaction of C_3S and tricalcium aluminate (C_3A) in OPC, increasing the exothermic rate, and strengthening particle flocculation [27,56,57].

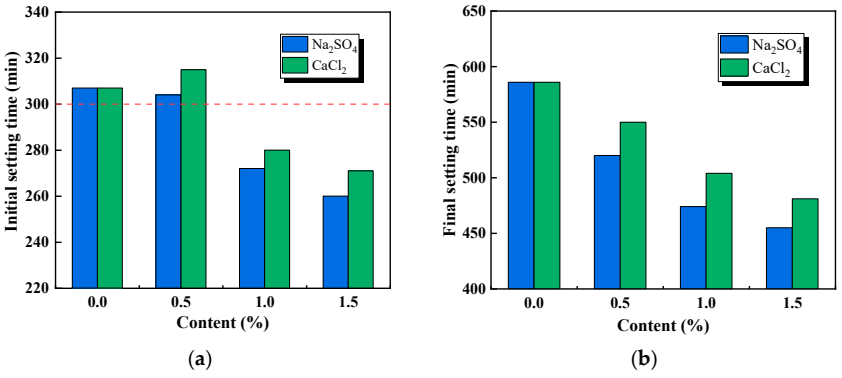


Figure 15. Setting time of MSWC-FSS with different early-strength agent content: (**a**) Initial setting time; (**b**) Final setting time.

4.2.3. Effect of Early-Strength Agents on the UCS of MSWC-FSS

Figure 16 shows the influence of different content of early-strength agents (Na_2SO_4 and $CaCl_2$) on the UCS of MSWC-FSS. With the increase of the content of the two kinds of early-strength agents, the UCS of MSWC-FSS at 3 and 7 days increased significantly, and the UCS of MSWC-FSS at 28 days increased first and then decreased, reaching the maximum at 1% content. Na_2SO_4 is better than $CaCl_2$ in enhancing the UCS of MSWC-FSS. In this study, the 28 day UCS of MSWC-FSS with all early-strength agent contents met the UCS requirements (>1 MPa) of Chinese standard DBJ51/T 188-2022 [41].

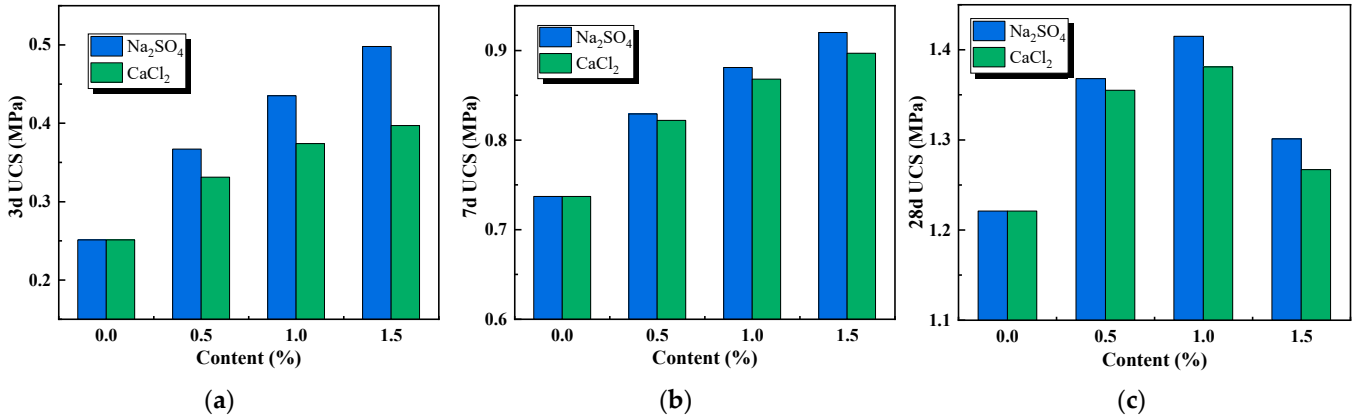


Figure 16. UCS of MSWC-FSS with different early-strength agent content: (**a**) Curing for 3 days; (**b**) Curing for 7 days; (**c**) Curing for 28 days.

There are differences in the mechanism of different early-strength agents promoting the early strength of MSWC-FSS is different. (1) Na_2SO_4 ionizes a large amount of $SO_{4^{2-}}$, promotes the dissolution of active SiO_2 and active Al_2O_3 in MSWC, promotes the conversion of C_3A to AFt, promotes the hydration reaction of MSWC, so as to improve the early strength of MSWC-FSS. (2) $CaCl_2$ reacts with C_3A to form calcium aluminate chloride hydration products. At the same time, $CaCl_2$ reacts with $Ca(OH)_2$ to form calcium chlorate precipitation. The dual action mechanism not only accelerated the hydration process of C_3A, but also significantly increased the solid content in MSWC-FSS through the in-situ precipitation of insoluble double salt compounds, and finally formed a three-dimensional microcrystalline skeleton structure with enhanced effect, which promoted the strength improvement.

The reasons for the adverse effects of excessive early-strength agent on the later strength are as follows. (1) The hydration products generated rapidly in a short time may lead to uneven crystal accumulation and loose bonding structure, increasing the internal porosity [1]. (2) The rapid precipitation of chemical products may form a barrier layer, which hinders the further hydration of internal MSWC particles [60]. (3) Aft has expansion effect, and the excessive formation of AFt may introduce internal stress, resulting in microcracks and local strength loss [56]. (4) The high concentration of $SO_{4^{2-}}$ can lead to chemical corrosion of cement-based hydrate and damage the microstructure integrity of FSS [27].

In general, the early-strength agent reduces the flow expansion, shortens the setting time, and significantly improves the early strength, but excessive addition has adverse effects on the long-term strength. The effects of two kinds of early-strength agents on the working and mechanical properties of MSWC-FSS are similar, but Na_2SO_4 plays a more significant role in promoting 3 d UCS. Considering the actual requirements and cost control of the project, it is considered that 1% Na_2SO_4 is the best choice for early-strength agent.

5. Sustainability Assessment of MSWC-FSS

5.1. Heavy Metal Leaching Behavior

Table 6 showed the results of heavy metal leaching test tests for the MSWC and MSWC-FSS. The leaching concentrations of various heavy metals in MSWC and MSWC-FSS were significantly lower than the limits specified in the Chinese standard GB.5085.3-2007 [43], indicating that MSWC would not cause heavy metal pollution. In addition, the leaching concentrations of various heavy metals in MSWC-FSS were much lower than those in MSWC, which reflected the immobilization effect of MSWC hydration products on heavy metal elements [61,62].

Table 6. Results of heavy metal leaching test of MSWC and MSWC-FSS.

Sample	Concentration (ug/L)								
	Zn	Cr	Cd	Cu	As	Pb	Ni	Mn	Hg
MSWC	223	Not detected	84.7	Not detected	5.3	4.2	Not detected	22.1	0.074
MSWC-FSS	87.4	Not detected	3.6	Not detected	2.2	1.1	Not detected	4.3	0.04
Limits	1×10^5	5×10^3	1×10^3	1×10^5	5×10^3	5×10^3	5×10^3	5×10^3	1×10^2

5.2. Cost and Carbon Emissions Analysis

The cost and carbon emissions of MSWC used for FSS had been evaluated and compared with OPC. Table 7 listed the life cycle inventory of MSWC, where the cost of raw materials was provided by solid waste suppliers and carbon emissions were referenced from published literature [15,63–65]. Based on the cost of raw materials, carbon emissions, and their proportion in MSWC, the cost of MSWC is calculated to be 25.09 $/ton, which is only 43.9% of the cost of OPC; The carbon emissions of MSWC are 186.20 kg/ton, which is only 22.4% of the carbon emissions from OPC.

Table 7. Life cycle inventory of MSWC.

Processes		Proportion in MSWC	Costs ($/ton)	CO_2 Emission (kg/ton)
Raw material procurement	OPC	20	57.14	830
	SS	20	14.29	15
	GBFS	40	21.43	19
	CFBFA	15	7.14	9
	DG	5	7.14	5
Manufacture	Mixing	100	0.80	8
MSWC		100	25.09	186.20

Based on the construction parameters in the on-site test, the cost and carbon emissions of MSWC and OPC required for preparing FSS were determined, as shown in Table 8. The density of FSS is 1.7 ton/m^3, the water-solid ratio is 0.45, and the cementitious material is 15%. Thus, the mass of cementitious material required for 1 m^3 FSS is calculated to be 0.176 tons. Furthermore, in practical engineering, the cost of MSWC required for 1 m^3 FSS was 4.41 $, and the carbon emission was 32.75 kg. The cost of OPC required for 1 m^3 FSS was 10.05 $, and the carbon emission was 145.97 kg. MSWC-FSS significantly reduce construction costs and carbon emissions, demonstrating notable economic and environmental benefits.

Table 8. Comparison of cost and carbon emission of MSWC and OPC in FSS.

Cementitious Material Type	FSS Density (ton/m^3)	Water-Solid Ratio	Cementitious Materials Content (%)	Cementitious Materials Mass (ton/m^3)	Unit-Cost ($/m^3)	Unit-CO_2 Emission (kg/m^3)
MSWC	1.7	0.45	15	0.176	4.41	32.75
OPC					10.05	145.97

6. Conclusions

This study developed a MSWC for FSS. Firstly, the influence of industrial solid waste contents on the UCS of MSWC-FSS was studied to determine the optimal mix proportion of MSWC. Then, the effects of two water reducers and two early-strength agents on the flow expansion, setting time, and UCS of MSWC-FSS were studied. Finally, the sustainability of MSWC-FSS was evaluated through heavy metal leaching test and economic and environmental benefits analysis. The following conclusions are obtained.

(1) With the increase of SS, GBFS, CFBFA and DG contents, the UCS of FSS increased first and then decreased. Considering the strength and the convenience of MSWC preparation, the optimal composition of MSWC is determined as SS:GBFS:CFBFA:DG:OPC = 20:40:15:5:20.

(2) With the increase of water reducer content, the flow expansion, setting time and UCS of MSWC-FSS added with PCE and FDN gradually increased. Compared with PCE, FDN has a slightly worse effect on improving the flow expansion of MSWC-FSS and a better effect on improving UCS. Both water reducers have adverse effects on the setting time. 0.5% of FDN is the best choice of water reducer for MSWC-FSS.

(3) With the increase of early-strength agent content, the flow expansion and setting time of MSWC-FSS added with Na_2SO_4 and $CaCl_2$ decreased, and the UCS of MSWC-FSS cured for 3 days and 7 days increased significantly, but the UCS of MSWC-FSS cured for 28 days first increased and then decreased. Compared with $CaCl_2$, Na_2SO_4 has more obvious effect on reducing the flow expansion and setting time of MSWC-FSS, and has better effect on improving UCS. 1% Na_2SO_4 is the best choice of early-strength agent for MSWC-FSS.

(4) The heavy metal leaching concentration of MSWC-FSS was far below the limit value and would not cause heavy metal pollution. The cost and carbon emissions of MSWC required for FSS were only 43.9% and 22.4% of those of OPC, respectively. MSWC-FSS was environmentally friendly, sustainable, and in line with clean production.

This study has preliminarily explored the material mix proportion, admixture compatibility and sustainability of MSWC-FSS, but there are still some limitations. It is suggested that more research should be carried out in the future on the influence of other kinds of admixtures (such as air entraining agent and retarder) and the compound effect of admixtures on the performance of MSWC-FSS.

Author Contributions: Conceptualization, X.C. and X.Z.; Methodology, H.S., R.S. and X.Z.; Formal analysis, H.M.; Investigation, H.M.; Resources, X.Y. and J.L.; Writing—original draft preparation, H.S.; Writing—review and editing, all authors; Visualization, H.S. and B.H.; Project administration, X.C. and R.S.; Funding acquisition, X.C., R.S. and X.Z. All authors have read and agreed to the published version of the manuscript.

Funding: This research was funded by the National Key R&D Program of China (grant number: 2022YFB2601900), Gansu Provincial Construction Science and Technology Project (grant number: JK2024-1), Shandong Provincial Natural Science Foundation (grant number: ZR2024LZN001), Scientific research projects of provincial enterprises supported by state-owned capital operating budget in Gansu Province (grant number: 2024GZ014), Lanzhou science and technology plan project (strong science and technology award supplement project) (grant number: 2024-8-37), Chongqing Natural

Science Foundation of China (grant number: CSTB2024NSCQ-LZX0044), National Natural Science Foundations of China (grant numbers: 52408465), Postdoctoral Innovation Talents Support Program (grant number: BX20240451), and China Postdoctoral Science Foundation (grant number: 2024M753850).

Data Availability Statement: The data that support the findings of this study are available from the corresponding author upon reasonable request.

Conflicts of Interest: Authors Rong Shu and Jilin Liu are employed by the Gansu Academy of Building Research (Group) Co., Ltd. Author Xiaoqing Yu is employed by the Jiangxi Ganyue Expressway Co., Ltd. The remaining authors declare that the research was conducted in the absence of any commercial or financial relationships that could be construed as a potential conflict of interest.

References

1. Cui, X.; Meng, H.; Liu, Z.; Sun, H.; Zhang, X.; Jin, Q.; Wang, L. Development, Performance, and Mechanism of Fluidized Solidified Soil Treated with Multi-Source Industrial Solid Waste Cementitious Materials. *Buildings* **2025**, *15*, 864. [CrossRef]
2. Lei, B.; Pang, S.; Xie, F.; Fan, H.; Sun, J. Optimization of ratios and strength formation mechanism of fluidized solidified soil from multi-source solid wastes. *J. Build. Eng.* **2025**, *108*, 112958. [CrossRef]
3. Yang, Q.; Zhang, N.; Han, L.; Shi, P.; Rong, Y.; Ba, M.; Li, S.; Miao, H.; Zhao, Y. Preparation and characterization of premixed fluidized solidified soil with municipal solid waste incineration bottom ash. *Constr. Build. Mater.* **2024**, *442*, 137541. [CrossRef]
4. Zhou, Y.; Zhang, R.; Yang, X.; Hou, L. The design methodology for proportioning fluidized solidified soil. *J. Build. Eng.* **2025**, *111*, 113127. [CrossRef]
5. Liu, S.; Zhan, J.; Wang, X. Influence of composition of curing agent and sand ratio of engineering excavated soil on mechanical properties of fluidized solidified soil. *Mater. Sci.-Pol.* **2023**, *41*, 57–67. [CrossRef]
6. Sun, X.; Liu, W.; Chen, X.; Wu, S.; Chen, G.; Bi, Y.; Chen, Z. Sustainable solutions: Transforming waste shield tunnelling soil into geopolymer-based underwater backfills. *J. Clean. Prod.* **2024**, *445*, 141363. [CrossRef]
7. Zhao, Y.; Zhang, N.; Chen, X. Test study on mechanical properties of compound municipal solid waste incinerator bottom ash premixed fluidized solidified soil. *Iscience* **2023**, *26*, 107651. [CrossRef]
8. Feng, T.; Lin, K.; Zhang, D.; Yu, Y.; Jiang, Y.; Jiang, P.; Li, N.; Wang, W. Fluidized solidified soil using construction slurry improved by fly ash and slag: Preparation, mechanical property, and microstructure. *Mater. Res. Express* **2024**, *11*, 115301. [CrossRef]
9. Liu, L.; Chen, S.; Chen, F.; He, L.; Shen, S. Analysis of strength characteristics and microstructure of alkali-activated slag cement fluidized solidified soil. *Mater. Res. Express* **2024**, *11*, 085502. [CrossRef]
10. Ma, Q.; Wang, K.; Li, Q.; Zhang, Y. Alkali-Activated Dredged-Sediment-Based Fluidized Solidified Soil: Early-Age Engineering Performance and Microstructural Mechanisms. *Materials* **2025**, *18*, 3408. [CrossRef]
11. Zhou, Y.; Huo, M.; Hou, L.; Chen, Z.; Zhang, L. Current Research and Prospect of Low Strength Flowable Filling Materials. *Mater. Rep.* **2024**, *38*, 130–138.
12. Scrivener, K.; Kirkpatrick, R. Innovation in use and research on cementitious material. *Cem. Concr. Res.* **2008**, *38*, 128–136. [CrossRef]
13. Bao, Z.; Cui, X.; Du, Y.; Jin, Q.; Hao, J.; Cao, T.; Li, X.; Zhang, X. Development and verification of subgrade service performance test system considering the principal stress rotation. *Transp. Geotech.* **2025**, *50*, 101474. [CrossRef]
14. Gu, F.; Xie, J.; Vuye, C.; Wu, Y.; Zhang, J. Synthesis of geopolymer using alkaline activation of building-related construction and demolition wastes. *J. Clean. Prod.* **2023**, *420*, 138335. [CrossRef]
15. Xie, J.; Zhang, J.; Cao, Z.; Blom, J.; Vuye, C.; Gu, F. Feasibility of using building-related construction and demolition waste-derived geopolymer for subgrade soil stabilization. *J. Clean. Prod.* **2024**, *450*, 142001. [CrossRef]
16. Peng, L.; Chen, B. Study on the basic properties and mechanism of waste sludge solidified by magnesium phosphate cement containing different active magnesium oxide. *Constr. Build. Mater.* **2021**, *281*, 122609. [CrossRef]
17. Yang, W.; Xue, Y.; Wu, S.; Xiao, Y.; Zhou, M. Performance investigation and environmental application of basic oxygen furnace slag—Rice husk ash based composite cementitious materials. *Constr. Build. Mater.* **2016**, *123*, 493–500. [CrossRef]
18. Lin, C.; Zhang, H.; Wang, C.; Chen, C.; Li, Z.; Zhang, J.; Li, Q.; Ma, W. Study on the mechanical properties and solidification mechanism of ground granulated blast furnace slag-carbide slag-desulfurization gypsum solidified shield musk. *Constr. Build. Mater.* **2025**, *475*, 141166. [CrossRef]
19. Wang, H.; Zhang, J.; Gu, F. Hydration mechanisms of geopolymer grouting materials derived from circulating fluidized bed fly ash and ground granulated blast furnace slag. *Powder Technol.* **2025**, *466*, 121402. [CrossRef]
20. Gao, Y.; Liu, X.; Li, Z.; Zhang, J. Effect of calcination process on ferrite phase and silicate phase of ferrite-belite-rich Portland cement clinker from industrial solid waste. *J. Sustain. Cem.-Based Mater.* **2024**, *13*, 145–163. [CrossRef]

21. Li, J.; Tian, B.; Li, X.; Wang, Z.; Cui, L.; Liang, D.; Wang, S.; Liu, Y.; Ou, H.; Liang, H. Energy effective utilization of circulating fluidized bed fly ash to prepare silicon-aluminum composite aerogel and gypsum. *Waste Manag.* **2023**, *172*, 162–170. [CrossRef] [PubMed]
22. Gao, W.; Zhou, W.; Lyu, X.; Liu, X.; Su, H.; Li, C.; Wang, H. Comprehensive utilization of steel slag: A review. *Powder Technol.* **2023**, *422*, 118449. [CrossRef]
23. Xiao, J.; Liu, J.; Xiang, J.; Liu, Z.; Liu, C.; Rong, Y.; Liu, Z.; Chang, J.; Zhang, H.; He, J. Optimization of Curing-agent Mix Ratio and Mechanism of Strength of Fluidized Multisource Solid-waste Solidified Loesses China J. *Highw. Transp.* **2025**, *38*, 250–263. [CrossRef]
24. Gu, Y.; Zhang, P.; Dong, W.; Sun, Q.; Yao, G.; Lv, R. Research on the preparation and properties of GBFS-based mud solidification materials. *Constr. Build. Mater.* **2024**, *423*, 135900. [CrossRef]
25. Al Jarmouzi, R.; Sun, Z.; Yang, H.; Ji, Y. The Synergistic Effect of Water Reducer and Water-Repellent Admixture on the Properties of Cement-Based Material. *Buildings* **2024**, *14*, 2734. [CrossRef]
26. Liu, J.; Yu, C.; Shu, X.; Ran, Q.; Yang, Y. Recent advance of chemical admixtures in concrete. *Cem. Concr. Res.* **2019**, *124*, 105834. [CrossRef]
27. Pang, C.; Tang, Z.; Yang, Z.; Huang, P. Early Strengthening Agent in Cementitious Composites and Its Function Mechanism: A Review. *Mater. Rep.* **2023**, *37*, 80–90.
28. Li, Y.; Liu, F.; Yu, F.; Du, T. A review of the application of steel slag in concrete. *Structures* **2024**, *63*, 106352. [CrossRef]
29. Gencel, O.; Karadag, O.; Oren, O.H.; Bilir, T. Steel slag and its applications in cement and concrete technology: A review. *Constr. Build. Mater.* **2021**, *283*, 122783. [CrossRef]
30. Connor, J.O.; Nguyen, T.B.T.; Honeyands, T.; Monaghan, B.; O'Dea, D.; Rinklebe, J.; Vinu, A.; Hoang, S.A.; Singh, G.; Kirkham, M.B.; et al. Production, characterisation, utilisation, and beneficial soil application of steel slag: A review. *J. Hazard. Mater.* **2021**, *419*, 126478. [CrossRef]
31. Kurniati, E.O.; Pederson, F.; Kim, H.-J. Application of steel slags, ferronickel slags, and copper mining waste as construction materials: A review. *Resour. Conserv. Recycl.* **2023**, *198*, 107175. [CrossRef]
32. Guo, J.; Bao, Y.; Wang, M. Steel slag in China: Treatment, recycling, and management. *Waste Manag.* **2018**, *78*, 318–330. [CrossRef] [PubMed]
33. Zhuang, S.; Wang, Q. Inhibition mechanisms of steel slag on the early-age hydration of cement. *Cem. Concr. Res.* **2021**, *140*, 106283. [CrossRef]
34. Jiang, Y.; Ling, T.-C.; Shi, C.; Pan, S.-Y. Characteristics of steel slags and their use in cement and concrete-A review. *Resour. Conserv. Recycl.* **2018**, *136*, 187–197. [CrossRef]
35. Gao, S.; Cui, X.; Ma, X.; Jin, Q.; Zhang, X.; Zeng, H. Experimental investigation on dynamic characteristics of hydrophobic modified silt after freezing-thawing under cyclic loading. *Cold Reg. Sci. Technol.* **2025**, *239*, 104606. [CrossRef]
36. Ma, X.; Kang, X.; Su, C.; Chen, Y.; Sun, H. Effects of water chemistry on microfabric and micromechanical properties evolution of coastal sediment: A centrifugal model study. *Sci. Total Environ.* **2023**, *866*, 161343. [CrossRef]
37. Ma, X.; Zhu, L.; Zou, X.; Kang, X. Investigation of the interface stick-slip friction behavior of clay nanoplatelets by molecular dynamics simulations. *Colloids Surf. A-Physicochem. Eng. Asp.* **2023**, *679*, 132601. [CrossRef]
38. Chen, Z.; Liu, J.; Li, R. Simulation and property prediction of MgO-FeO-MnO solid solution in steel slag. *Mater. Lett.* **2020**, *273*, 127930. [CrossRef]
39. *JTG 3430*; Test Methods of Soils for Highway Engineering. Ministry of Transport of the People's Republic of China: Beijing, China, 2020.
40. *ASTM D6103*; Standard Test Method for Flow Consistency of Controlled Low Strength Material (CLSM). American Society for Testing and Materials: West Conshohocken, PA, USA, 2017.
41. *DBJ51/T 188*; Technical Standard for Engineering Application by Using Premixed Fluidized Stabilized Soil. Department of Housing and Urban Rural Development of Sichuan Province: Chengdu, China, 2022.
42. *GB/T 1346*; Test Methods for Water Requirement Of Standard Consistency, Setting Time and Soundness of the Portland Cement. State Administration for Market Regulation, National Standardization Administration: Beijing, China, 2024.
43. *GB 5085.3*; Identification Standards for Hazardous Wastes-Identification For Extraction Toxicity. Ministry of Ecology and Environment of the People's Republic of China: Beijing, China, 2007.
44. *HJ/T 300*; Solid Waste-Extraction Procedure for Leaching Toxicity-Acetic Acid Buffer Solution Method. Ministry of Ecology and Environment of the People's Republic of China: Beijing, China, 2007.
45. Lu, C.; Shen, Q.; Zhang, Z.; Zhang, X.; Hawileh, R. Synergistic effect of waste steel slag powder and fly ash in sustainable high strength engineered cementitious composites: From microstructure to macro-performance. *J. Build. Eng.* **2025**, *113*, 114039. [CrossRef]
46. Chang, L.; Cui, S.; Wang, J.; Liu, H.; Zhou, B. Enhancing the hydration activity of steel slag-Portland cement composite by BES sodium activator. *Sustain. Chem. Pharm.* **2025**, *48*, 102213. [CrossRef]

47. He, H.; Gao, Y.; Yu, J.; Zhang, W.; Shen, X.; Zhang, M. Municipal solid waste incineration fly ash as activator for ground granulated blast-furnace slag: Hydration behavior and stabilization/solidification effectiveness. *Case Stud. Constr. Mater.* **2025**, *23*, e05177. [CrossRef]
48. Zhou, M.; Chen, P.; Chen, X.; Ge, X.; Wang, Y. Study on hydration characteristics of circulating fluidized bed combustion fly ash (CFBCA). *Constr. Build. Mater.* **2020**, *251*, 118993. [CrossRef]
49. Zhang, S.; Shi, T.; Ni, W.; Li, K.; Gao, W.; Wang, K.; Zhang, Y. The mechanism of hydrating and solidifying green mine fill materials using circulating fluidized bed fly ash-slag-based agent. *J. Hazard. Mater.* **2021**, *415*, 125625. [CrossRef] [PubMed]
50. Ke, G.; Li, Z.; Jiang, H. Study on long-term solidification of all-solid waste cementitious materials based on circulating fluidized bed fly ash, red mud, carbide slag, and fly ash. *Constr. Build. Mater.* **2024**, *427*, 136284. [CrossRef]
51. Cerato, F.; Rocha, J. Effect of heat-treated flue gas desulfurization gypsum on the setting time of stabilized mortars: An experimental study. *J. Build. Eng.* **2025**, *111*, 113240. [CrossRef]
52. Wang, Y.; Bao, L.; Wang, J.; Yao, T.; Sun, G.; Zong, C.; Zhang, H. Effect of fluorgypsum and flue gas desulfurization gypsum on properties of aluminate cement based grouting materials. *Constr. Build. Mater.* **2025**, *493*, 143319. [CrossRef]
53. Wang, W.; Huang, Y.; Wang, S.; Peng, G.; Wang, H. Experimental study on influence of plasticizer on fluidity of convection solidified silt Chin. *J. Geotech. Eng.* **2024**, *46*, 1605–1612.
54. Zhang, T.; Wang, Z.; Wang, W.; Li, G.; Guo, H.; Zhang, H. Property enhancement and mechanism of cement-based composites from the perspective of nano-silica dispersion improvement. *Case Stud. Constr. Mater.* **2025**, *22*, e04125. [CrossRef]
55. Jin, L.; Song, W.; Shu, X.; Huang, B. Use of water reducer to enhance the mechanical and durability properties of cement-treated soil. *Constr. Build. Mater.* **2018**, *159*, 690–694. [CrossRef]
56. Li, G.; Zhang, J.; Niu, M.; Song, Z. The mechanism of alkali-free liquid accelerator on the hydration of cement pastes. *Constr. Build. Mater.* **2020**, *233*, 117296. [CrossRef]
57. Wu, Z.; Zhang, W.; Huang, W.; Pan, Y.; Wang, J.; Zhou, H.; Li, Z. Synergistic Effect of Early-Strength Agents on the Mechanical Strength of Alkali-Free Liquid Accelerator Mortar. *J. Mater. Civ. Eng.* **2024**, *36*, 04024178. [CrossRef]
58. Xie, M.; Wang, Z.; Yin, L.e.; Li, H. Research on Synergistic Enhancement of UHPC Cold Region Repair Performance by Steel Fibers and Early-Strength Agent. *Buildings* **2025**, *15*, 2630. [CrossRef]
59. Zhao, Y.; Zhao, Y.; Zhu, Z.; Chen, G.; Wu, H.; Liu, C.; Gao, J. Effect of a novel negative temperature early-strength agent in improving concrete performance under varying curing temperatures. *Case Stud. Constr. Mater.* **2024**, *21*, e03748. [CrossRef]
60. Yang, Y.; Yang, Z.; Cheng, Z.; Zhang, H. Effects of wet grinding combined with chemical activation on the activity of iron tailings powder. *Case Stud. Constr. Mater.* **2022**, *17*, e01385. [CrossRef]
61. Gao, W.; Ni, W.; Zhang, Y.; Li, Y.; Shi, T.; Li, Z. Investigation into the semi-dynamic leaching characteristics of arsenic and antimony from solidified/stabilized tailings using metallurgical slag-based binders. *J. Hazard. Mater.* **2020**, *381*, 120992. [CrossRef]
62. Wang, H.; Ju, C.; Zhou, M.; Chen, J.; Dong, Y.; Hou, H. Sustainable and efficient stabilization/solidification of Pb, Cr, and Cd in lead-zinc tailings by using highly reactive pozzolanic solid waste. *J. Environ. Manag.* **2022**, *306*, 114473. [CrossRef]
63. Jeon, I.K.; Azzam, A.; Al Jebaei, H.; Kim, Y.-R.; Aryal, A.; Baltazar, J.-C. Effects of alkali-activated slag binder and shape-stabilized phase change material on thermal and mechanical characteristics and environmental impact of cementitious composite for building envelopes. *J. Build. Eng.* **2023**, *76*, 107296. [CrossRef]
64. Shi, Y.; Long, G.; Ma, C.; Xie, Y.; He, J. Design and preparation of ultra-high performance concrete with low environmental impact. *J. Clean. Prod.* **2019**, *214*, 633–643. [CrossRef]
65. Tran, T.M.; Trinh, H.T.M.K.; Nguyen, D.; Tao, Q.; Mali, S.; Pham, T.M. Development of sustainable ultra-high-performance concrete containing ground granulated blast furnace slag and glass powder: Mix design investigation. *Constr. Build. Mater.* **2023**, *397*, 132358. [CrossRef]

Disclaimer/Publisher's Note: The statements, opinions and data contained in all publications are solely those of the individual author(s) and contributor(s) and not of MDPI and/or the editor(s). MDPI and/or the editor(s) disclaim responsibility for any injury to people or property resulting from any ideas, methods, instructions or products referred to in the content.